ANL/ET/CP--90022
CONF-9607126--5

DENSE CERAMIC MEMBRANES FOR METHANE CONVERSION*

U. Balachandran, R. L. Mieville, and B. Ma
Energy Technology Division
Argonne National Laboratory
Argonne, IL 60439

C. A. Udovich
Amoco Exploration/Production
Naperville, IL 60566

May 1996

Manuscript for invited presentation at 1st Joint Power and Fuel Systems Contractors' Conference, July 9-11, 1996, Pittsburgh, PA.

*Work at ANL is supported by the U.S. Department of Energy, Pittsburgh Energy Technology Center, under Contract W-31-109-Eng-38.

DISCLAIMER

DENSE CERAMIC MEMBRANES FOR CONVERTING METHANE TO SYNGAS

U. BALACHANDRAN, R. L. MIEVILLE, AND B. MA
ENERGY TECHNOLOGY DIVISION
ARGONNE NATIONAL LABORATORY
9700 SOUTH CASS AVENUE
ARGONNE, IL 60439-4838

C. A. UDOVICH
AMOCO EXPLORATION/PRODUCTION
NAPERVILLE, IL 60566

Introduction

This report focuses on a mechanism for oxygen transport through mixed-oxide conductors as used in dense ceramic membrane reactors for the partial oxidation of methane to syngas (CO and H_2). The in-situ separation of O_2 from air by the membrane reactor saves the costly cryogenic separation step that is required in conventional syngas production.

The mixed oxide of choice is $SrCo_{0.5}FeO_x$, which exhibits high oxygen permeability and has been shown in previous studies to possess high stability in both oxidizing and reducting conditions (1); in addition, it can be readily formed into reactor configurations such as tubes.

An understanding of the electrical properties and the defect dynamics in this material is essential and will help us to find the optimal operating conditions for the conversion reactor. In the meantime, it may also give us some clues for developing better materials.

In this paper, we discuss the conductivities of the $SrFeCo_{0.5}O_x$ system that are dependent on temperature and partial pressure of oxygen (pO_2). Based on the experimental results, a defect model is proposed to explain the electrical properties of this system. The oxygen permeability of $SrFeCo_{0.5}O_x$ is estimated by using conductivity data and is compared with that obtained from methane conversion reaction (1).

This defect model includes normal oxygen sites, interstitial oxygen ions, and vacancies and electron holes, together with metal ions of variable valence. The concentration of a given variable-valence ion is determined by the partial pressure of oxygen, pO_2. At high pO_2, higher valence states exist while at low pO_2, low valence ions dominate.

A mixed-conducting oxide can be considered in which oxygen ions and electrons or corresponding lattice defects are mobile. When the sample is placed in an oxygen potential gradient, oxygen ions will move from high pO_2 to low pO_2. The current density of oxygen ion produced by oxygen potential gradient is given by (2)

$$\vec{j}(x) = -\frac{\sigma_{tot} t_{ion} t_{el}}{4F} \, grad \, \tilde{\mu}(pO_2), \qquad (1)$$

where $\tilde{\mu} = \tilde{\mu}_0 + RT\ln(pO_2)$ is the chemical potential of oxygen, F is Faraday's constant, σ_{tot} is the total conductivity, and transference t_{ion} and t_{el} are the ionic and electronic numbers respectively. The charged particles will move according to the driving force, $grad\ \tilde{\mu}(pO_2)$.

If we integrate over the thickness of the membrane, on both sides of Eq. 1, the current density of the oxygen ions flowing through the membrane can be calculated. Thus, the oxygen permeability of the membrane can be obtained by using

$$J_{O_2} = -\frac{RT}{16F^2L}\int_{pO2(0)}^{pO2(x)} \sigma_{tot} t_{ion} t_{el} d\ln(pO_2), \qquad (2)$$

where R is the gas constant, L the membrane thickness, and J_{O_2} is oxygen permeability, mol cm^{-2} s^{-1} through the membrane. Here, σ_{tot}, t_{ion}, and t_{el} are functions of temperature and pO_2 in general.

Experimental

Samples were prepared from $SrFeCo_{0.5}O_X$ powder, which in turn was made from $SrCo_3$, $Co(NO_3)_2 \cdot 6H_2O$, and Fe_2O_3 in the manner described in Ref. 1. Construction and operation of the gas-tight electrochemical cell and the experimental assembly for measuring high-temperature conductivity is described in Ref. 3.

Results and Discussion

Conductivities in Air

By using the conventional four-probe method and the electron-blocking four-probe method, we were able to measure the total and ionic conductivities in air directly. Because total conductivity is the sum of electronic conductivity and ionic conductivity, the electronic conductivity can be calculated by subtracting ionic conductivity from total conductivity. The conductivities and ionic transference number (t_i) are plotted in Fig. 1 as a function of temperature. It was found that the total, electronic, and ionic conductivities all increase with increased temperature. The ionic transference number is almost independent of temperature. At 800°C, total and ionic conductivities are 17 and 7 S cm^{-1}, respectively. Activation energies of electron holes and oxygen ions are 0.40 and 0.37 eV, respectively, as determined by Arrhenius type plots. Furthermore, the ionic transference number of $SrFeCo_{0.5}O_X \approx 0.4$ in the experimental temperature region (625 to 975°C).

Unlike most of the oxide conductors, the ionic and electronic conductions contribute almost equally to the electrical properties of this sample. $SrFeCo_{0.5}O_X$ is really a mixed conductor in air. Also unlike other materials, the Sr(Fe,Co)Ox system (3-5), the oxide ion activation energy of 0.37 eV for $SrFeCo_{0.5}O_X$ is much lower. This means that bonding of oxygen ions to the lattice is much weaker and thus oxygen ions can move more easily in $SrFeCo_{0.5}O_X$ than in other systems.

The oxygen diffusion coefficient (8.9×10^{-7} cm^2/s at 900°C) results of $SrFeCo_{0.5}O_x$, which we reported earlier, confirms this conclusion (4).

Conductivity as a Function of pO_2

Figure 2 shows the pO_2 dependence of total, ionic, and electronic conductivities and the ionic transference number of $SrFeCo_{0.5}O_x$ at 850°C. Based on conductivity behavior, the entire experimental pO_2 range can be divided into five regions. Within each of these regions, conductivities of $SrFeCo_{0.5}O_x$ behave differently.

The pO_2-dependent behaviors of $SrFeCo_{0.5}O_x$ can be understood by introducing the concept of trivalence-to-divalence transition of Fe ions into the sample. In the $SrFeCo_{0.5}O_x$ sample, we have two variable-valence metal ions, Fe and Co. In the temperature and pO_2 range of our experiment, Co ions are most likely in the divalent state, and Fe ions can have a trivalent-to-divalent transition when pO_2 is reduced. The Fe^{3+} to Fe^{2+} transition in $SrFeCo_{0.5}O_x$ under the reduced oxygen environment can be represented in the notation of Kroger (6):

$$2Fe_{Fe}^{\bullet} + O_O^{\times} \leftrightarrow 2Fe_{Fe}^{\times} + V_O^{\bullet\bullet} + 1/2\, O_2 \qquad (3)$$

or in a simple way as

$$Fe_{Fe}^{\bullet} + e' \leftrightarrow Fe_{Fe}^{\times}, \qquad (4)$$

where $Fe_{Fe}^{\bullet}$ and $Fe_{Fe}^{\times}$ correspond to the trivalent and divalent Fe ions. The electroneutrality relationship should now be written as

$$n + 2[O_i^{''}] = p + 2[V_O^{\bullet\bullet}] + [Fe_{Fe}^{\bullet}], \qquad (5)$$

where n is the concentration of electrons, $O_i^{''}$ of oxygen interstitial ions, $V_O^{\bullet\bullet}$ of oxygen vacancies, P of electron holes, and $Fe_{Fe}^{\bullet}$ of ions one valence higher than $Fe_{Fe}^{\times}$.

Estimated equilibrium coefficients can be made from Eqs. 3-5, based on certain assumptions. This allows us to define boundaries for five regions where thermodynamic stability occurs for different sets of ions.

Based on our defect model, the trivalence-to-divalence transition should occur near the boundary of regions II and III. At high pO_2, the concentrations of oxide ions ($O_i^{''}$) and holes ($Fe_{Fe}^{\bullet} = h^{\bullet}$) are much higher than those of oxygen vacancies ($V_O^{\bullet\bullet}$) and electrons (e'); the conductivity behaviors are dominated by $O_i^{''}$ and $h^{\bullet}$. In region I, $[O_i^{''}]$ and p decrease while $[V_O^{\bullet\bullet}]$ and n increase with decreased pO_2. Although the slopes for $[O_i^{''}]$ and p are the same (both $\approx 1/6$, the mobility of holes is greater than that of interstitial oxygen ions), so electronic conductivity changes more rapidly than does ionic conductivity. This is why we see an increase in the ionic transference number with decreased pO_2 in this region.

In region II, the concentrations of $h^{\bullet}$ and e' do not change, and the concentrations of $O_i^{''}$ and $V_O^{\bullet\bullet}$ change more rapidly, with slopes of 1/2 and -1/2, respectively. This leads to a more rapid change in ionic conductivity than in electronic conductivity. Hence, the ionic transference number decreases with decreased pO_2 and reaches its minimum at the boundary of regions II and III.

In region III, similar to the case in region I, $[O_i^{''}]$ and p have the same slope, as do $[V_O^{\bullet\bullet}]$ and n; unlike the case in region I, we have $[O_i^{''}] \geq [V_O^{\bullet\bullet}]$ and $p \geq n$ here. Again, because the mobilities of electrons and holes are greater than these of oxygen ions and vacancies, electronic conductivity (which should equal to the sum of electron and hole conductivities under this circumstance) decreases more rapidly than does ionic conductivity with decreased pO_2. Thus, we observed an increase in ionic transference number.

In region IV, the so-called mixed-conduction zone, $[O_i^{''}]$ and $[V_O^{\bullet\bullet}]$ are independent of pO_2, p decreases while n increases with the decreasing in pO_2, ionic conductivity does not change while the electronic conductivity first decreases, reaches its minimum, and then increases. Thus, we observed a maximum in ionic transference number corresponding to the minimum in electronic conductivity, which accurred at the point where concentrations of electrons and holes are equal. In region V, $[V_O^{\bullet\bullet}] >> [O_i^{''}]$ and $n >> p$, where the oxygen vacancies and electrons are the dominant charge carriers. Although the slopes of $[V_O^{\bullet\bullet}]$ and n are the same because the mobility of electrons is greater than that of oxygen vacancies, electronic conductivity increases more rapidly than ionic conductivity, and the ionic transference number decreases with decreased pO_2. Finally, the ionic transference number reaches a value of ≈0.3 at $\log(pO_2) = -16$.

The region boundaries of the $SrFeCo_{0.5}O_X$ sample, along with the phase transition boundaries of cobalt oxide and ferro oxides, are plotted in Fig. 3 as a function of the reciprocal temperature. We can see that $Co_3O_4 \rightarrow 3CoO + 0.5O_2$ occurred beyond the I-II boundary, $3Fe_2O_3 \rightarrow 2Fe_3O_4 + 0.5O_2$ occurred in region III, and that $Fe_3O_4 \rightarrow 3FeO + 0.5O_2$ occurred beyond region V. This confirms the assumption we made while building our defect model. The trivalence-to-divalence transition of Fe ions governed the electrical properties of the $SrFeCo_{0.5}O_X$ when pO_2 is reduced.

Oxygen Permeability

The pO_2 dependence of total and ionic conductivities has been measured in our experiment. Although we do not know the details of the oxygen potential distribution inside the sample, as long as we know σ_{tot} and σ_{ion} as functions of pO_2, the thickness of the $SrFeCo_{0.5}O_X$ reactor membrane and the pO_2 on each side of the membrane, we can use Eq. 2 to calculate (by numerical integration) the permeability of oxygen penetrating the reactor membrane.

Calculated oxygen permeabilities as a function of temperature are plotted in Fig. 4, along with oxygen permeation data obtained from a methane conversion reactor. They agree with each other within a factor of 2 to 3, and they are two orders higher than the oxygen permeability of other compositions in the $(La,Sr)(Fe,Co)O_X$ system (7). However, a significant difference in

activation energies exists between calculated and experimental values. This is probably due to much lower pO_2 in the experimental reactor conditions (log $pO_2 \approx -22$).

Conclusions

By using a gas-tight electrochemical cell with flowing air as the reference environment, we were able to produce an oxygen partial pressure (pO_2) as low as 10^{-16} atm in the cell. Total and ionic conductivities of $SrFeCo_{0.5}O_x$ were measured with the conventional four-probe and electron-blocking four-probe methods at various pO_2 levels. At 800°C in air, the total and ionic conductivities of $SrFeCo_{0.5}O_x$ are 17 and 7 S cm^{-1}, respectively, and the ionic transference number is 0.4. The activation energy of oxide ions is 0.37 eV in air. The pO_2 dependence of the electrical conductivity behavior of the $SrFeCo_{0.5}O_x$ system is quite complex. Conductivities, and thus ionic transference number, behave differently in five regions when pO_2 is reduced from that of ambient air to 10^{-16} atm. However, with the defect model we proposed, in which the trivalence-to-divalence transition of Fe ions has been taken into consideration, we can understand this system quite well. In the high-pO_2 range, interstitial oxygen ions and holes are the dominant charge carriers, while in the low-pO_2 range, oxygen vacancies and electrons are the dominant charge carriers.

References

1. U. Balachandran, J. T. Dusek, S. M. Sweeney, R. L. Mieville, P. S. Maiya, M. S. Kleefisch, S. Pei, T. P. Kobylinski, and A. C. Bose, *Proc. 3rd Int. Conf. on Inorganic Membranes*, Y. H. Ma, ed. pp. 229, Worcester, MA (1994).
2. H. L. Tuller, "Mixed Conduction in Nonstoichiometric Oxides," in Nonstoichiometric Oxides, Materials Science Series, O. T. Sorensen, ed., pp. 271, Academic Press, New York (1981).
3. B. Ma, U. Balachandran, J-H. Park, and C. V. Segre, J. Electrochem. Soc 143, 1724 (1996).
4. B. Ma, U. Balachandran, J.-H. Park, and C. U. Segre, *Solid State Ionics*, **83** (1996; in press).
5. K. Nisancioglu and T. M. Gur, *Solid State Ionics*, **72**, 199 (1994).
6. F. A. Kroger, "The Chemistry of Imperfect Crystals," North-Holland Publishing Co., Amsterdam, Nethrlands (1964).
7. H. Kruidhof, H. J. M. Bouwmeester, R. H. E. Doorn, and A. J. Burggraf, *Solid State Ionics*, **63**, 816 (1993).

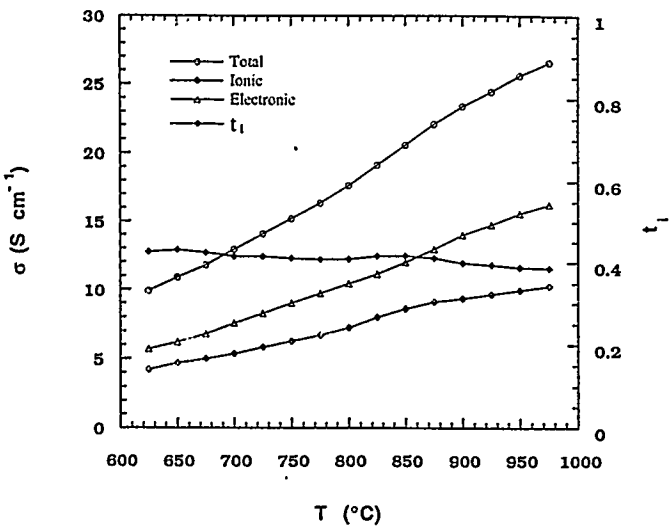

Fig. 1. Temperature dependence of conductivities, corresponding to left y-axis; and ionic transference number (t_i), corresponding to right y-axis of $SrFeCo_{0.5}O_x$ in air.

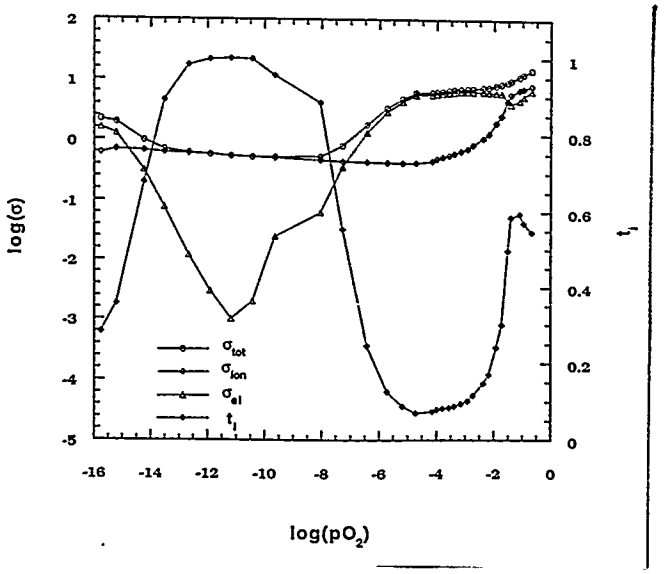

Fig. 2. Oxygen partial pressure dependence of total, ionic, and electronic conductivites, corresponding to left y-axis; and ionic transference number, corresponding to right axis, at 850°C.

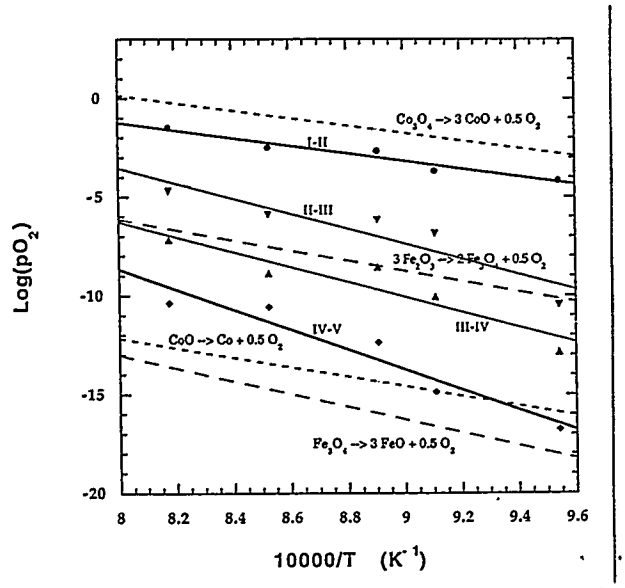

Fig. 3. Transition boundaries of $SrFeCo_{0.5}O_x$, together with phase transitions of cobalt and ferro oxides.

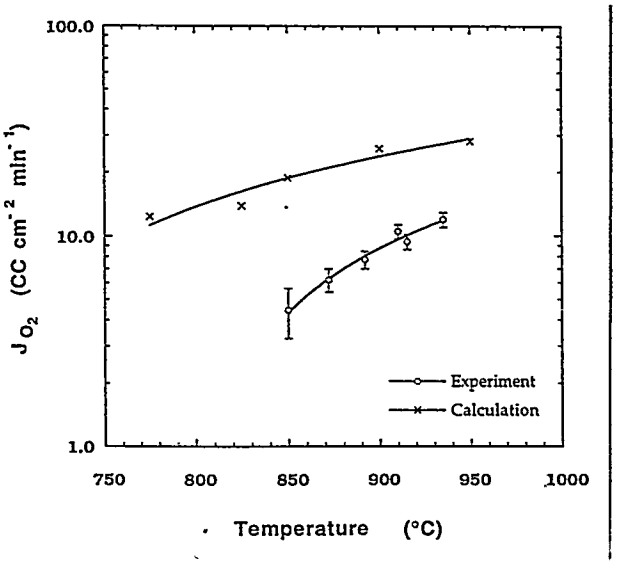

Fig. 4. Temperature dependence of oxygen flux rate obtained from methane conversion reactor experiment and that calculated from conductivity data (calculation) for $SrFeCo_{0.5}O_x$.